Gold solubility in the common gold-bearing minerals: Experimental evaluation and application to pyrite

Article *in* European Journal of Mineralogy · November 1999

CITATIONS
50

READS
246

1 author:

Vladimir Tauson
Russian Academy of Sciences
136 PUBLICATIONS **822** CITATIONS

SEE PROFILE

Eur. J. Mineral.
1999, **11**, 937-947

Gold solubility in the common gold-bearing minerals: Experimental evaluation and application to pyrite

VLADIMIR L. TAUSON*

A.P. Vinogradov Institute of Geochemistry, Siberian Branch of Russian Academy of Sciences, 664033 Irkutsk, Favorski street 1a, Russia

Abstract: A method is proposed for determining gold solubility in the common gold-bearing minerals (sulfides, *etc.*) using so-called "gold-assisting elements" (GAE). These elements increase gold solubility in the fluid phase, enabling minerals formed from hydrothermal fluids to be saturated with gold. Two experimental approaches are discussed: (1) identifying the solid-solution limit of gold in a mineral structure by determining the maximum content of uniformly distributed gold constituent which remains unchanged with increasing gold content in the coexisting fluid phase, and (2) determining the gold distribution between the mineral under study and a reference mineral with a sufficiently high and well-defined solid-solution limit of gold and utilizing the phase composition correlation principle. Statistical treatment of analytical data for single crystals permits inference of the structurally bound gold constituent. Greenockite (α-CdS) incorporates a maximum of 50 ± 7 ppm Au in solid solution at 500°C and 1 kbar and this is used as a reference mineral to determine gold solubility in pyrite under the same conditions in the presence of As and Se as gold-assisting elements. The value obtained for gold solubility in pyrite (3 ± 1 ppm Au) is in reasonable agreement with the results of ion-probe microanalysis of natural pyrites. The data suggest that monovalent gold substitutes for divalent iron, giving rise to an acceptor center compensated by a donor defect, either a sulphur vacancy or a hydrosulphide ion replacing S_2^{2-}.

Key-words: gold solubility, pyrite, greenockite, hydrothermal experiments.

Introduction

Experimental and natural data on gold solubility in the common gold-bearing minerals (pyrite, galena, sphalerite, *etc.*) are rather contradictory. Pyrite is one of the most important concentrators of gold. For example, Kurauti (1941) prepared pyrite crystals allegedly containing over 2,000 ppm Au and reported that the unit-cell edge of pyrite decreases with increasing Au content. Spectrographic analysis at the time showed gold to be apparently distributed uniformly throughout the pyrite, but it has been ascertained that when pyrite and gold are co-precipitated, the pyrite crystals are impregnated with discrete submicroscopic gold particles (Tyurin, 1965). Thus, such conventional spectrographic analysis is not suitable. Mironov & Geletiy (1978) synthesized Au-containing pyrite crystals hydrothermally in the presence of radioactive ^{195}Au and concluded that gold is not structurally bound but occurs as microinclusions at the boundaries of crystals. The gold content in solid solution was estimated to be ≤ 0.01 ppm, the declared minimum detection limit of the autoradiographic method. Thus, the experimental data on gold solubility in pyrite span five orders of magnitude of Au concentration. Such a discrepancy is also characteristic of natural pyrites, and "there is as yet no direct evidence of solid solution gold in pyrite" (Dunn *et al.*, 1989). The gold contents in

*e-mail: vltauson@igc.irk.ru

0935-1221/99/0011-0937 $ 2.75

pyrites of various genetic types are rarely over 1 ppm, although the samples from Witwatersrand (South Africa) and some other localities contain as much as ~170-260 ppm (Cambel *et al.*, 1980). As a rule gold contents over 100 ppm are associated with arsenian pyrite (Cook & Chryssoulis, 1990; Fleet *et al.*, 1993). However, in many cases Au occurs as finely dispersed particles distributed zonally with As (Mao, 1991), one explanation being that this is the result of decomposition of a metastable solid solution $Fe(S,As)_2$ that initially contained gold as an isomorphic admixture (Fleet *et al.*, 1989; Arehart *et al.*, 1993). Fleet & Mumin (1997) suggested that "invisible gold" in arsenian pyrite represents Au removed from ore fluids by chemisorption at As-rich, Fe-deficient surface sites that was incorporated into the crystals in metastable solid solution. Nevertheless, As-doped pyrite can also play an electrochemical role, acting as a cathode accumulating gold in metallic form (Möller, 1994).

Hydrothermal synthesis may still prove to be a promising method for studying gold solubility in pyrite. Nevertheless, direct co-crystallization of pyrite and gold by a process similar to that described by Mironov & Geletiy (1978) may be undesirable for two reasons. Firstly, the implicit assumption that the isomorphous gold concentration in pyrite is a maximum when gold particles are present within the crystals or at crystal boundaries may not be applicable to crystallization from a coexisting fluid that is saturated with gold. It is now known that discrete crystals and thin films of gold may be located at specific sites on the pyrite substrate, showing a marked affinity for surface defects; the native gold is precipitated by reduction-driven chemisorption at the pyrite-electrolyte interface (Starling *et al.*, 1989; Mycroft *et al.*, 1995; Scaini *et al.*, 1997). Physical defects such as fractures and etch pits are the active sites for gold nucleation. These defects can give rise to gold precipitation from fluids both undersaturated or very slightly supersaturated with respect to Au^0. Möller (1994) confirmed that gold can be extracted electrochemically even from undersaturated solutions. Secondly, the native gold cannot be considered as a reference state for gold in the pyrite structure, because its solubility is dependent upon the fluid composition. The end member of the theoretical solid solution series AuS_2 with a pyrite-type structure is unknown. There is no evidence that gold microinclusions located on the pyrite crystal faces originated from this compound or from any other gold sulfide decomposed at the pyrite-fluid interface.

The present article is concerned with the study of gold solubility in pyrite using a novel experimental approach.

Background

The problem of determination of the proportion of structurally bound gold may be solved in at least two ways: (1) saturation of investigated minerals with gold using so-called "gold-assisting" elements (GAE), and (2) study of Au partitioning between coexisting minerals. In the first method the GAE raise gold solubility in the fluid phase and lead to co-crystallization of the mineral and gold *via* the formation of intermediate Au- and GAE-containing compounds (Tauson & Smagunov, 1997). To determine the solubility limit of gold under given P,T-conditions we firstly find the maximum Au-content uniformly distributed throughout the mineral. The uniformity criterion may then be introduced empirically with the data on synthetic isomorphous mixtures taken into account (Tauson *et al.*, 1998). The most probable maximum value of the coefficient of variation (C_i) of structurally bound gold concentration was assumed to be 20 % ($\mathbf{C_i = \frac{S_i}{\bar{x}_i} \cdot 100}$ %, where S_i is the root-mean-square deviation, and $\bar{x}_i$ is the arithmetic mean, see Shaw, 1969). The presence of other gold constituents significantly elevates the C_i value. For example, the presence of non-structurally bound Au in pyrite and pyrrhotite can increase C_i up to 120-180 % (Tauson & Smagunov, 1997).

The second way of determining the proportion of structurally bound gold involves the study of gold partitioning between coexisting minerals (Perchuk & Riabchikov, 1976). Experiments are conducted both in the regime where the minerals are undersaturated with gold (low Au contents in the fluid phase owing to small GAE amounts added to the system) and in the regime of higher Au and GAE contents. A schematic diagram of the correlation of phase composition under constant P,T-conditions and varying GAE contents is shown in Fig. 1. The mineral pair consists of the mineral being investigated and a reference mineral with a sufficiently high and well-defined solid solution limit of gold. When the experimental system contains minor amounts of GAE, the gold concentrations are also low and the prevalent gold constituent is structurally bound. Line I in Fig. 1 is representative of this scenario and referred to as the "true phase composition correlation" (Tauson,

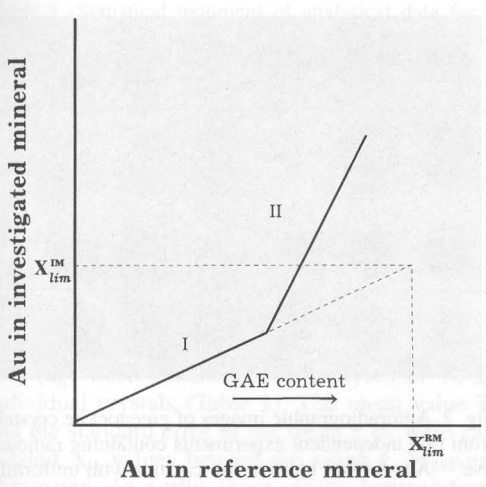

Fig. 1. Schematic representation at constant P,T conditions of gold distribution between coexisting reference mineral and the mineral under investigation as a function of GAE content. Line I corresponds to "true phase composition correlation" and line II corresponds to "apparent phase composition correlation". X^{IM}_{lim} and X^{RM}_{lim} are the incorporation limits of gold in investigated mineral and in reference mineral, respectively (see text for further discussion).

1989a). Adhering to the aforementioned 20 % C_i criterion, the scatter of experimental points along this line must be relatively low. Increasing the GAE content leads to an increase in the gold concentration in the fluid phase and gives rise to the formation of gold constituents that are not structurally bound. So line II in Fig. 1 can be referred to as the line in the diagram of "apparent phase composition correlation" (Tauson, 1989a). This line represents a tendency for regular and appropriate changes in compositions of coexisting phases owing to a specific correlation in the behaviour of gold constituents not incorporated into the structures of crystals. For instance, the correlation may be attributed to adsorption of Au-containing intermediate compounds in proportion to the change of Au concentration in the coexisting fluid phase.

In principle and for low concentrations, the solid-solution limit (or the solubility) of gold in the investigated mineral (X^{IM}_{lim}) could be found at the extension of line I in the point corresponding to the solid-solution limit of Au in the reference mineral (X^{RM}_{lim}), as shown in Fig. 1. Therefore, the solid-solution limit may be estimated by the following expression: $X^{IM}_{lim} = X^{RM}_{lim} \cdot \frac{1}{K^{RM/IM}_{SBAu}}$, where $K^{RM/IM}_{SBAu}$ is the distribution coefficient of structurally bound Au constituent between the reference and investigated minerals. Possible curvature of line I owing to nonideality of gold solid solutions in minerals is neglected in this first approximation.

It is evident that line I in Fig. 1 passes through the origin, whereas line II generally does not, because the apparent phase composition correlation does not satisfy Henry's law. Attributing experimental points to one or another line (I or II) in questionable cases may be clarified using the coefficients of variation of gold content.

The second way of determining the proportion of structurally bound gold is most effective in the case of a low solubility limit of gold in the mineral being studied. This is due to the problem of evaluation of structurally bound Au when in the presence of its other forms, which usually are much more abundant. As we shall see later, this is indeed the case for pyrite.

The method proposed gives no direct evidence that Au is structurally bound. When using the second approach, we can determine the gold constituent which is uniformly distributed and satisfies Henry's law as structurally bound gold. Therefore, it is highly probable that this constituent actually represents the solid-solution gold. Additional methods should be used for the determination of the valence state and incorporation mechanism of gold. Unfortunately, no direct quantitative method is available at this time for such a low-concentration level.

Experimental study of gold solubility in reference mineral

A convenient reference mineral for the study of gold solubility in sulfides is greenockite (α-CdS), a phase which contains up to approximately 100 ppm of structurally bound gold (Mironov *et al.*, 1987). Below we will test the validity of these data using the approach considered in the beginning of the previous section.

Experimental procedure

Greenockite crystals were synthesized hydrothermally in the presence of Au and GAE's As and Se. The experiments (similar to those of Tauson & Smagunov, 1997) were conducted in stainless steel pressure vessels (autoclaves). Starting chemicals were contained in a rigid, thick-walled, inner vessel with an approximately 50 ml capacity, machined from titanium alloy VT-

6 (Ti + ~6 wt%Al + ~5 wt%V). The vessels were held in boiling HNO_3 before each run. Complete sealing of the vessel was attained using a conical closure and a fire-resistant steel thrust ring, taking advantage of the difference in thermal expansivities of the materials (Tauson & Akimov, 1991). Cadmium sulfide was transported across a temperature gradient of 0.4 K/cm (over 25 cm) which was measured on the outer autoclave wall. A pressure of 1 kbar was fixed to within ± 10 % by the amount of the solution added to the inner vessel, balanced by the amount of water added to the outer vessel. The starting materials were pure reagent grade CdS, CdSe, or As. The experiments were carried out at 500°C for 10 days in two stages: a 3 day isothermal stage and a 7 day non-isothermal stage with a temperature of 500°C at the top and 510°C at the bottom of the inner vessel. Ammonium chloride was used to accelerate the transport reaction rate. Gold was added to a 7 % aqueous NH_4Cl solution in the form of radioactive ^{195}Au aqua regia solution. NaOH was added to neutralize the acids just before the vessel was sealed. The total concentration of salts was 10 wt% in each experiment. Experiments were terminated by removing the pressure vessel from the furnace and quenching in cold water. The quenching rate was measured by Tauson & Akimov (1986) to be ~5 degrees per second and was quite enough for saving the crystals formed during the experiment.

Several runs were conducted using a special titanium sampler fixed with a pin junction in the upper part of the inner vessel. The sampler enables a portion of high-temperature fluid to be trapped during cooling of the autoclave for the subsequent determination of gold concentrations in the fluid phase coexisting with the mineral phase (Tauson & Smagunov, 1997).

These experiments represent unreversed syntheses, and require attention to the degree to which equilibrium is approached. Comparison of the results of isothermal and gradient experiments in sulfide systems may be made using the data of Bethke & Barton (1971), Geletiy *et al.* (1979), and Tauson & Chernyshev (1981). Nonisothermal hydrothermal experiments are appropriate at temperatures ≥ 400°C and sufficiently low gradients. These conditions were fulfilled in this study.

Analytical methods

A quantitative method, combining autoradiography and atomic absorption analysis, has been developed to try to determine gold in solid solution in greenockite. Fig. 2 shows the computer images of autoradiograms obtained under identical conditions from greenockite crystals containing radioactive ^{195}Au. Two sets of crystals from independent experiments 1 and 2 are presented. The uniform darkening is attributed to gold in solid solution, whereas the dark spots correspond to inclusions of Au-containing particles. The grains designated with arrows in Fig. 2 reveal a uniform Au distribution and so can be used to estimate structurally bound Au both by chemical analysis and darkening density. This combined analytical technique was confirmed using perfect, facetted CdS crystals, absolutely free of small particles deposited during quenching (a very important condition as these particles contain high amounts of adsorbed gold). Several crystals, usually the largest, reveal some kind of zoning in Au distribution (Fig. 2). These specific crystals were not used in obtaining the final results. The optimum crystal size is found to be about 1-2 mm.

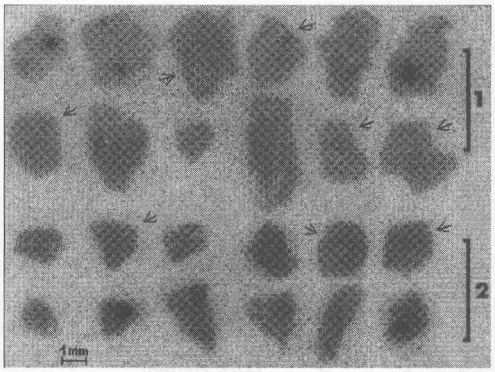

Fig. 2. Autoradiographic images of greenockite crystals from two independent experiments containing radioactive ^{195}Au. Arrows indicate the crystals with uniformly distributed Au.

The gold contents in single crystals of CdS were determined after dissolution of each crystal in hot HCl by graphite furnace AAS (detection limit 0.2 ppb, precision ± 10 %), using freshly prepared, matrix-matched standards. All measurements were performed using a Perkin-Elmer Model 503 atomic absorption spectrometer equipped with D_2 background corrector, and HGA-72 graphite furnace. The crystals analysed were generally about 1-2 mm in diameter. It was ascertained that reliable results could be obtained for a number of single crystals in complete agreement with the autoradiographic crystal selection technique. Initial estimates of the gold concentra-

Table 1. Statistical treatment of analytical data for 4 batches of CdS crystals containing ~50 ppm Au in solid solution from the same run (Au contents in ppm).

No. of crystals analysed	$\bar{x}_1(\pm\sigma_1)$	$\bar{x}_2$	$\bar{x}_3(\pm\sigma_3)$	n_3*
10	67.8(26.9)	58.0	48.2(9.5)	7
15	72.4(21.4)	60.5	49.4(5.5)	9
20	70.3(14.3)	59.6	53.7(5.6)	13
25	65.7(10.9)	57.9	53.1(4.7)	16

*No. of analyses in final sample.

tion (x_{il}) were obtained from analyses of 10-25 individual crystals (Table 1). The mean value $\bar{x}_1$ and the standard error of the mean $\pm \sigma_1$ were calculated. x_{i1} values beyond the range $\pm 2\sigma_1$ were eliminated. As a rule, these values deviated from the mean $\bar{x}_1$ to higher gold contents, owing to the presence of inclusions of Au-containing phases (Fig. 2). The remainder x_{i2}, with the mean $\bar{x}_2$, was tested with the one-sided criterion $\frac{x_{i2}^{+} - \bar{x}_2}{\bar{x}_2} \leq 0.2$ consistent with the aforementioned 20 % maximum value C_i for structurally bound Au. The subset of x_{i2} values not satisfying this condition were rejected on the assumption that the crystals were contaminated with adsorbed Au-containing intermediate compounds (Tauson & Smagunov, 1997). The residual x_{i3} with the mean $\bar{x}_3$ (Table 1) is thus assumed to best describe structurally bound Au. The standard error $\pm \sigma_3$ of the mean $\bar{x}_3$ was interpreted as the error of the determination of structurally bound Au concentration. This procedure provides sufficient reproducibility (about $\pm$ 10 %) for representative initial samples containing more than 15 analyses (Table 1).

Experimental results

In the experiments we obtained greenockite crystals up to 3 mm in diameter. The crystals have a pinkish-brown or orange-brown colour and well-developed faces belonging to the common hexagonal forms. Increasing concentrations of Se or As gave rise to a red tint, and mixed crystals Cd(S,Se) rich in CdSe were dark-red to black. We have synthesized Cd(S,Se) solid solutions within the composition range $Cd(S_{0.88}\ Se_{0.12})$-CdSe (Table 2), where the concentrations of structurally bound Au changed only slightly. The coexisting fluid contained up to approximately 12 ppm Au, and the bulk gold contents in Cd(S,Se) mixed crystals increased with Au concentration in the fluid phase (the apparent phase composition correlation, see above). As seen from Table 2, the limit of gold substitution in greenockite at 500°C and 1 kbar is equal to ~50 ppm. This is the approximate maximum content of uniformly distributed gold produced even when the gold content in the coexisting fluid phase is further increased. In respect of Au incorporation into CdS, the data obtained using As as GAE are similar to those for Se (Table 2). The solubility of gold in pure greenockite can be obtained by extrapolation of the Au content to zero concentration of GAE (Tauson *et al.*, 1998) to avoid any influence on the solid-solution limit of gold by the GAE. Linear extrapolation gives 48 ppm Au for Se and 52 ppm Au for As, with an average of 50 ppm; thus, the difference is within

Table 2. Results of experimental study of gold solubility in a reference mineral (greenockite) in the presence of radioactive ^{195}Au and gold- assisting elements (As and Se) at 500°C and 1 kbar in 7 % NH_4Cl solution.

Run No.	Charge composition (wt%)			Products	Au (ppm)	
	CdS	CdSe	As		crystals*	fluid**
1	100	-	-	Gr	21	3
2	75.1	24.9	-	GrCs(12)	46	7
3	53.1	46.9	-	GrCs(33)	49	9
4	33.5	66.5	-	GrCs(60)	51	11
5	-	100	-	Cs	50	12
6	99.3	-	0.7	Gr	51	5
7	99.0	-	1.0	Gr	48	5
8	98.0	-	2.0	Gr	49	7
9	96.5	-	3.5	Gr	58	8
10	94.6	-	5.4	Gr	59	13

Note: Gr is greenockite; Cs = cadmoselite (CdSe), GrCs = greenockite-cadmoselite solid solutions (mol% CdSe in parentheses).

* Structurally bound Au estimated by graphite furnace AAS for autoradiographically selected crystals.

** Rough estimate based on the analysis of high-temperature solution trapped nonisothermally with a sampler (see Tauson & Smagunov, 1997, for details).

Table 3. Results of experimental study of gold distribution between pyrite and greenockite in the presence of GAE (As and Se) at 500°C and 1 kbar in 10 % NH_4Cl solution.

Run No.	Charge composition						Products	Au (ppm) ($\pm 1\sigma_3$)*	
	S/Fe, at.ratio	weight percent						Gr	Py
		CdS	Fe+S	As	Se	Au			
11	2.4	30	68.98	0.02	-	1	Gr,Py	20.2(5.4)	1.2(0.4)
12	2.5	30	68.9	0.1	-	1	Gr,Py	26.0(7.2)	2.1(0.9)
13	2.7	30	68.9	0.1	-	1	Gr,Py,S°	30.1(6.8)	1.3(0.5)
14	2.5	30	68.8	0.2	-	1	Gr,Py	38.3(6.3)	1.9(0.3)
15	2.7	30	68.8	0.2	-	1	Gr,Py,S°	39.1(7.0)	1.5(0.4)
16	2.5	30	68.7	0.3	-	1	Gr,Py	40.5(9.6)	2.5(0.5)
17	3.0	30	68.7	0.3	-	1	Gr,Py,S°	42.8(6.5)	2.0(0.7)
18	2.5	30	68.6	0.4	-	1	Gr,Py	53.7(5.6)	6.4(0.8)
19	2.5	30	68.3	0.7	-	1	Gr,Py	58.7(12.2)	4.5(1.7)
20	2.5	30	68.0	1.0	-	1	Gr,Py	72.1(11.6)	6.2(2.0)
21	2.5	30	67.0	2.0	-	1	Gr,Py	81.2(10.7)	4.2(1.3)
22	3.0	30	68.98	-	0.02	1	Gr,Py,S°	24.3(5.8)	1.0(0.4)
23	2.5	30	68.9	-	0.1	1	Gr,Py	34.0(6.4)	2.2(0.4)
24	2.5	30	68.8	-	0.2	1	Gr,Py	39.8(5.8)	2.5(0.7)
25	2.5	30	68.7	-	0.3	1	Gr,Py	41.7(4.2)	2.7(0.6)
26	3.0	30	68.7	-	0.3	1	Gr,Py,S°	57.6(7.2)	1.7(0.8)
27	2.5	30	68.6	-	0.4	1	Gr,Py	59.0(7.1)	3.5(0.6)
28	2.3	30	68.5	-	0.5	1	Gr,Py	82.6(16.8)	5.2(2.6)

Note: Gr is greenockite, Py = pyrite, S° = native sulphur. Native gold is present in all runs in the charge.
* Graphite furnace AAS analysis of 15-20 single crystals of both sulfides from each run followed by a procedure to evaluate structurally bound gold content (see text for more details).

the limits of analytical error (± 10%). Thus, it seems reasonable to conclude from this study that the solubility of gold in greenockite at 500°C and 1 kbar is 50 ± 7 ppm Au.

Evaluation of gold solubility in pyrite

Greenockite and pyrite were crystallized together at 500°C and 1 kbar from hydrothermal solution containing 10 wt% NH_4Cl. The experimental procedure was the same as that employed to study greenockite. Sulfide starting materials consisted of CdS and extremely pure metallic iron and elemental sulphur. GAE was added to the charge as elemental Se or As, and thin gold foil was used as a source of gold. The total amount of starting materials in the charge was 7 g in each experiment.

In the experiments we obtained greenockite and pyrite crystals up to 3 and 5 mm in diameter, respectively. Greenockite crystals were pinkish-brown to dark brown, due to iron. The iron contents in greenockite crystals were determined by flame AAS using a Perkin-Elmer Model 403 atomic absorption spectrometer. The concentrations were found to be 0.1–0.7 wt% Fe (precision 10 %). Therefore, Fe contents were insignificant because the experiments were conducted close to the liquid sulphur stability field.

Only the most perfect crystals with clean faces were analyzed for gold using graphite furnace AAS (see above). Greenockite crystals were dissolved in HCl and pyrite crystals in $HCl+KClO_3$, both under heating. The analytical data obtained were treated with the statistical procedure mentioned above to estimate structurally bound gold. The data are given in Table 3 and in Fig. 3. Minor amounts of GAE give rise to structurally bound Au in both greenockite and pyrite, providing the system "pyrite-greenockite" behaves in the manner of true phase composition correlation. Gold tends to partition into greenockite; the distribution coefficient is $K_{SBAu}^{Gr/Py} \cong 18 \pm 5$ (weight proportions) assuming Henry's law. The limit of solid-solution gold in pyrite under these conditions can be estimated as 3 ± 1 ppm (Fig. 3). It is noteworthy that no discernible difference exists between the runs utilizing different GAE (As or Se). However, the data obtained in the presence of elemental sulphur show an appreciable shift to lower gold concentrations in pyrite (Fig. 3). The corresponding value of $K_{SBAu}^{Gr/Py}$ under these conditions is higher (23 ± 5), but the difference is within the limits of error. We can only speculate about the tendency for lower

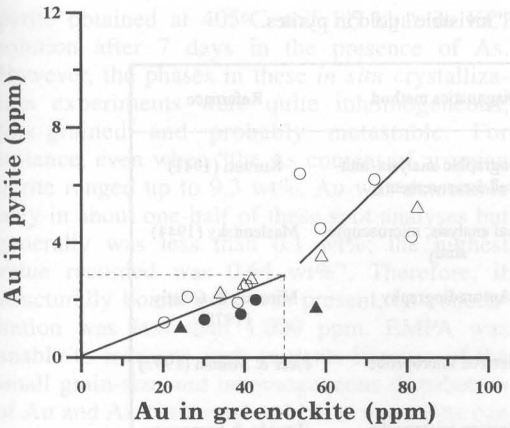

Fig. 3. Experimental gold distribution between pyrite and greenockite in the presence of the gold assisting elements As and Se at 500°C and 1 kbar. Graphic estimate of gold solubility in pyrite indicated by dotted lines (see text for more details). Open circles and triangles show the data obtained for coexisting Py and Gr in the presence of As and Se, respectively. Solid circles and triangles show the data obtained for coexisting Py, Gr and S° in presence of As and Se, respectively.

Au contents at higher sulfur fugacities. Increasing amounts of GAE enhance gold contents both in the investigated mineral (pyrite) and in the reference mineral (greenockite). However, the experimental data scatter significantly along the line representing the apparent phase composition correlation beyond the limit of Au incorporation into the reference mineral. A further feature of note is that the coefficients of variation of gold content are markedly higher in this region as compared with the region where greenockite is undersaturated with gold (Table 3). The GAE contents in greenockite and pyrite crystals as obtained by graphite furnace AAS are shown in Table 4. It is suggested that in the region where true phase composition correlation is obeyed (line I in Fig. 1 along which the phases are undersaturated with gold), the concentration of uniformly distributed Au is equal to the concentration of structurally bound Au (structural gold represents a prevailing gold constituent in mineral crystals, see above). Accordingly, in the region beyond the solid-solution limits, the difference in concentrations between uniformly distributed and structurally bound gold represents the contribution of intermediate Au- and GAE-containing compounds to the apparent phase composition correlation (Tauson & Smagunov, 1997). Table 4 clearly shows the absence of a correlation between structural gold and GAE contents. However, we can infer that GAE correlate with the gold constituent owing to adsorbed Au. This is likely to be valid for greenockite, not for pyrite, presumably because CdS is a stronger adsorbant of intermediate compounds in comparison to pyrite.

Table 4. Gold and GAE contents in greenockite and pyrite crystals.

Mineral	Run No.	Gold concentration (ppm)				GAE (wt%)	
		Total ($\bar{x}_1$)	Uniformly distributed($\bar{x}_3$)	Structurally bound	UD - SB*	As	Se
Greenockite	12	85.9	26.0	26.0	0	0.007	-
	14	44.6	38.3	38.3	0	0.005	-
	18	65.7	53.7	50.0	3.7	0.006	-
	19	93.2	58.7	50.0	8.7	0.011	-
	21	88.9	81.2	50.0	31.2	0.013	-
	23	35.3	34.0	34.0	0	-	0.155
	24	58.8	39.8	39.8	0	-	0.230
	26	80.1	57.6	50.0	7.6	-	0.366
Pyrite	12	9.9	2.1	2.1	0	0.018	-
	14	2.7	1.9	1.9	0	0.008	-
	18	34.4	6.4	3.0	3.4	0.003	-
	19	11.7	4.5	3.0	1.5	0.006	-
	21	6.0	4.2	3.0	1.2	0.012	-
	23	8.9	2.2	2.2	0	-	0.098
	24	17.3	2.5	2.5	0	-	0.086
	26	15.0	1.7	1.7	0	-	0.272

*Difference in concentrations between uniformly distributed and structurally bound gold which represent the contribution of intermediate Au- and GAE-containing compounds to apparent phase composition correlation

Table 5. Maximum contents of "invisible" gold in pyrites.

Max Au (ppm)	Sample origin	Diagnostics method	Reference
2,000	Synthetic, conditions uncertain	Spectrographic analysis, unit-cell measurements	Kurauti (1941)
~300	Synthetic, ~400°C	Chemical analysis, microscopic study	Maslenitsky (1944)
≤0.01	Synthetic, 500°C and 1 kbar	Autoradiography	Mironov & Geletiy (1978)
3,700	Synthetic, 405°C and 1.5 kbar, in presence of As	Electron microprobe	Fleet & Mumin (1997)
550±300; ≤200*	Synthetic, 450°C and 1 kbar, in presence of As and Se	Electron microprobe	Tauson & Smagunov (1997)
4.5	Natural, Canadian sulfide deposits	Combined technique of ion-probe microanalysis, secondary ion mass spectrometry and ion implantation	Chryssoulis *et al.* (1987)
5.1±2.9**	Natural, mainly Canadian deposits (12 objects)	"	Cook & Chryssoulis (1990)
6.8	Natural, 46 pyrite grains from Trout Lake, Flin Flon, Manitoba	Ion microprobe	Healy & Petruk (1990)
3.0-4.5	Natural, 42 pyrite samples from Moblin deposit, Northwestern Quebec	"	Larocque *et al.* (1995)
3±1*	Synthetic, 500°C and 1 kbar	Atomic absorption analyses of individual crystals	This work

*Structurally bound Au only.
**Zoned arsenian pyrites of Olympias and Elmtree deposits are eliminated because of strong probability of metastable solid solutions $Fe(As,S)_2$ providing metastable gold solubility (Fleet *et al.*, 1989; Arehart *et al.*, 1993). Also neglected is the isolated value of 20 ppm from the Congress ore containing only negligible amount of 'invisible" gold (1.2±0.6 ppm).

Discussion

Table 5 lists the data on maximum contents of "invisible gold" in pyrites of different origin. In addition to synthetic pyrites, several natural samples are presented for which the gold contents (obtained with ion-probe microanalysis) are known from the literature. Electron and proton microprobe data for natural pyrites were not taken into account, because of the relatively high detection limits (200 ppm and 15-20 ppm, respectively). For example, pyrites from Australian volcanic-hosted massive sulfide deposits, studied by Huston *et al.* (1995) using a proton microprobe, contained as much as 50-210 ppm Au, but only 4-14 per cent of the analyses showed contents > MDL (minimum detection limit), so the character of Au distribution is unclear. As seen from Table 5, the experimental data of the present work are inconsistent with the data of some of the previous investigators on synthetic pyrites. It may be inferred from this study that the main reason for the discrepancy between the data of different authors lies in the analytical problem of separating the gold constituent that is structurally bound from the more abundant constituents of "invisible gold". This problem cannot be solved with the conventional methods used by Kurauti (1941), Maslenitsky (1944), Tyurin (1965), *etc.* Although electron microprobe analysis (EMPA) is also unsuitable for this purpose, this method provided evidence that gold solubility in pyrite is less than 200 ppm (Tauson & Smagunov, 1997). Fleet & Mumin (1997) determined 3,700 ppm Au in

pyrite obtained at 405°C and 1.5 kbar in KCl solution after 7 days in the presence of As. However, the phases in these *in situ* crystallization experiments were quite inhomogeneous, fine-grained and probably metastable. For instance, even when "the As content of arsenian pyrite ranged up to 9.3 wt%, Au was detectable only in about one-half of these spot analyses but generally was less than 0.1 wt%; the highest value recorded was 0.64 wt%". Therefore, if structurally bound gold was present, its concentration was less than 1,000 ppm. EMPA was unable to measure such contents because of the small grain-size and inhomogeneous distribution of Au and As. Structural gold concentrations can be determined by autoradiographic methods in combination with atomic absorption analysis. Even though they used a sufficiently sensitive autoradiographic method, Mironov & Geletiy (1978) underestimated gold solubility in pyrite crystals at 500°C and 1 kbar, because they were unable to control the saturation of the fluid phase and coexisting pyrite with gold. On the other hand, the data obtained in this work appear to be in reasonable agreement with the results of ion-microprobe studies of natural samples (Table 5), affording the conclusion that ion-probe microanalysis can provide accurate estimates of the solid-solution gold in natural pyrites.

The chemical state of "invisible gold" in pyrite and the mechanisms of valence compensation remain uncertain (Fleet & Mumin, 1997). Gold incorporation into the pyrite structure is treated in two main ways. First, trivalent gold may substitute for Fe^{2+} with the imbalance of charge satisfied by the paired dianion AsS^{3-} replacing S_2^{2-} in the anionic sublattice (Cook & Chryssoulis, 1990). Second, monovalent gold may substitute for Fe^{2+}, with the compensating centers or electron vacancy centers created along the S-S bond (Zhang *et al.*, 1987). Both mechanisms are possible from a crystal-chemical standpoint, as are many others. However, the coupled substitution $Au^{3+} \leftrightarrow F^{2+}$, $AsS^{3-} \leftrightarrow S_2^{2-}$ does not appear feasible, because volume compensation is lacking (*i.e.* volume effects of this substitution are positive in both sublattices). ^{197}Au Mössbauer spectroscopic study (Marion *et al.*, 1991) showed that gold in pyrite does not have the same chemical environment as gold in arsenopyrite. In the second case, although bond lengths do not differ significantly (Fe^{2+} - S = 2.26 Å and Au^{+} - S = 2.30 Å; Liao & Schwarz, 1994), the nature of the compensated center is unknown. Bokiy & Bondar (1979) have demonstrated the possibility of hydrogen incorporation into natural pyrite as an HS^- anion, and this mechanism has been invoked to explain morphological features of hydrothermally grown pyrite crystals (Tauson, 1989b). The heterogeneous reaction of hydrogen ion exchange between pyrite (Py) and a fluid phase (Fl) may be written

$$S_2^{2-}(Py) + H^+(Fl) = HS^-(Py) + 1/2\ S_2\ (Fl), \quad (1)$$

or under alkaline conditions

$$S_2^{2-}(Py) + OH^-\ (Fl) + 1/2O_2(Fl) = HS^-\ (Py) + SO_2\ (Fl). \quad (2)$$

The possibility of the coupled substitution $Au^+ \leftrightarrow Fe^{2+}, HS^- \leftrightarrow S_2^{2-}$ is supported by the formation of metastable Au- and H-containing iron sulfide below 200°C (Kozerenko *et al.*, 1986). The presence of H-containing species is also confirmed by a proton magnetic resonance study. Kozerenko *et al.* (1986) interpreted their results in favor of an OH^- anion, but the technique they used was not able to distinguish OH^- from HS^-- species.

Our experiments on gold solubility in pyrite imply that the mechanism involving As is inoperative, because the solid-solution limit of gold is independent of the type of gold-assisting element (As or Se). These elements reveal a sufficiently different crystal-chemical behavior in pyrite (Tauson & Smagunov, 1997), and the compatibility of two data sets obtained separately using As and Se provides evidence that the limit of Au solution in pyrite is independent of arsenic substitution for sulphur. This is also supported by the data of Table 4, showing the absence of a correlation between structural gold and GAE contents. On the other hand, the results obtained under higher sulphur fugacity (in equilibrium with liquid sulphur) probably support Eqn.1. This equilibrium actually shifts to the left under increasing f_{S_2}, in accordance with Le Chatelier's rule. Therefore, Au incorporation into the pyrite structure is suppressed in equilibrium with liquid sulphur, and this is not in conflict with experimental evidence (Fig. 3, Table 3). Nevertheless, Au^+ substitution for Fe^{2+} in the pyrite structure (the acceptor centre Au'_{Fe}) may be compensated not only by HS^- substituting S_2^{2-} (the donor centre $HS_S^{\cdot}$) but also by donor defect $\square_S$, the anionic vacancy (Voitzechovskiy *et al.*, 1975). In any case, Au solubility must be lower under extremely high sulphur fugacity, for which the concentrations of $\square_S$ and $HS_S^{\cdot}$ are at a minimum.

Conclusions

A method is proposed for determining gold solubility in the common gold-bearing minerals.

Its components are (1) saturation of the mineral with a structurally bound gold constituent in the presence of gold-assisting elements that raise gold solubility in the crystal growth medium, and (2) study of the gold distribution between the mineral investigated and a reference mineral with a sufficiently high and well-defined incorporation limit of gold. Statistical treatment of the analytical data for single crystals makes it possible to reasonably infer the structurally bound gold constituent.

Greenockite (α–CdS) is found to be a convenient reference mineral to determine gold solubility in pyrite. The value obtained for gold solubility in pyrite, 3 ± 1 ppm Au at 500°C and 1 kbar, is in poor agreement with previously determined experimental values which vary up to five orders of magnitude. Early investigators (Kurauti, 1941; Maslenitsky, 1944, *etc.*) overestimated gold solubility in pyrite, because they used methods with low spatial resolution. Although current methods afford better estimates, Mironov & Geletiy (1978) underestimated the gold incorporation limit because they did not saturate the fluid phase (and coexisting pyrite) with gold.

Among the data on natural pyrites, only the results of ion-probe microanalysis appear to be in reasonable agreement with the present experimental data on structurally bound gold.

The mechanism of gold incorporation into pyrite usually invoked to explain gold enrichment in pyrite presupposes the coupled substitution $Au^{3+} \leftrightarrow Fe^{2+}$, $AsS^{3-} \leftrightarrow S_2^{2-}$, but this mechanism seems to be highly improbable based on the present experimental study. The results of the experiments are consistent with the inference that monovalent gold substitutes for divalent iron, giving rise to an acceptor center compensated by a donor defect, either a sulphur vacancy or a hydrosulphide ion replacing S_2^{2-}.

Acknowledgements: Thanks are due to Dr. Anatoly G. Mironov and Ms. Natalia G. Bugaeva of the Geological Institute (Ulan-Ude) for their assistance in the autoradiographic study of crystals containing radioactive gold. Mrs. Taisa M. Pastushkova and Mrs. Olga I. Bessarabova are thanked for their help with analysis. A review by Dr. Richard O. Sack of Purdue University contributed significantly to the preparation of this paper. An anonymous EJM's reviewer offered many useful comments. The work is supported by the Russian Foundation for Fundamental Research, Grant 96-05-64644.

References

Arehart, G.B., Chryssoulis, S.L., Kesler, S.E. (1993): Gold and arsenic in iron sulfides from sediment-hosted disseminated gold deposits: Implication for depositional processes. *Econ. Geol.*, **88**, 171-185.

Bethke, P.M. & Barton, P.B., Jr. (1971): Distribution of some minor elements between coexisting sulfide minerals. *Econ. Geol.*, **66**, 140-163.

Bokiy, G.B. & Bondar, A.M. (1979): On hydrogen role in structures of sulfides. *Doklady Akademii Nauk, SSSR*, **248**, 956-959 (in Russian).

Cambel, B., Stresko, V., Skerencakova, O. (1980): The contents of gold in pyrites of various genesis. *Geol. Carpatica*, **31**, 139-159.

Chryssoulis, S.L., Cabri, L.J., Salter, R.S. (1987): Direct determination of invisible gold in refractory sulphide ores. *Proceedings of International Symposium on Gold Metallurgy* (Winnipeg, 1987.). Vol.1 , 235-244.

Cook, N.J. & Chryssoulis, S.L. (1990): Concentrations of "invisible gold" in the common sulfides. *Can. Mineral.*, **28**, 1-16.

Dunn, J.G., Graham, J., Just, J., Nguyen, G., Avraamides, J. (1989): The roasting and leaching of refractory sulphides. *Proceedings of Mineralogy-Petrology Symposium* (Sidney, 1987), 97-99.

Fleet, M.E., MacLean, P.J., Barbier, J. (1989): Oscillatory-zoned As-bearing pyrite from strata-bound and stratiform gold deposits: An indicator of ore fluid evolution. *Econ. Geol. Monograph* **6**, 356-362.

Fleet, M.E., Chryssoulis, S.J., Mac Lean, P.J., Davidson, R., Weisener, C.G. (1993): Arsenian pyrite from gold deposits: Au and As distribution investigated by SIMS and EMP, and color staining and surface oxidation by XPS and LIMS. *Can. Mineral.*, **31**, 1-17.

Fleet, M.E. & Mumin, A.H. (1997): Gold-bearing arsenian pyrite and marcasite and arsenopyrite from Carlin Trend gold deposits and laboratory synthesis. *Am. Mineral.*, **82**, 182-193.

Geletiy, V.F., Chernyshev, L.V., Pastushkova, T.M. (1979): Cadmium and manganese distribution between galena and sphalerite. *Geologia Rudnykh Mestorozhdenii*, **6** , 66-75 (in Russian).

Healy, R.E., & Petruk, W. (1990): Petrology of Au-Ag-Hg alloy and "invisible" gold in the Trout Lake massive sulfide deposit, Flin Flon, Manitoba. *Can. Mineral.*, **28**, 189-206.

Huston, D.L., Sie, S.H., Suter, G.F., Cooke, D.R., Both, R.A. (1995): Trace elements in sulfide minerals from Eastern Australia volcanic-hosted massive sulfide deposits: Part I. Proton microprobe analyses of pyrite, chalcopyrite, and sphalerite, and Part II. Selenium levels in pyrite: Comparison with $\delta^{34}S$ values and implications for the source of sulfur in volcanogenic hydrothermal systems. *Econ. Geol.*, **90**, 1167-1196.

Kozerenko, S.V., Tuzova, A.M., Rodionova, I.M., Kuznetsova, T.P., Kalinichenko, A.M., Ivanitsky,

V.P. (1986): On one of the mechanisms of formation of finely-dispersed gold in iron sulfides. *Geokhimiya*, **12**, 1706-1714 (in Russian).

Kurauti, G. (1941): Synthetic study of gold-containing pyrite. *Suiyokway-Si*, **10**, 419-424 (not seen; extracted from *Chemical Abstracts*, **35**, 3563).

Larocque, A.C.L., Hodgson, C.J., Cabri, L.J., Jackman, J.A. (1995): Ion-microprobe analysis of pyrite, chalcopyrite and pyrrhotite from the Mobrun VMS deposit in Northwestern Quebec: Evidence for metamorphic remobilization of gold. *Can. Mineral.*, **38**, 373-388.

Liao, M.S. & Schwarz, W.H.E. (1994): Effective radii of the monovalent coin metals. *Acta Cryst.*, **B 50**, 9-12.

Mao, Shui He (1991): Occurrence and distribution of invisible gold in a Carlin-type gold deposits in China. *Am. Mineral.*, **76**, 1964-1972.

Marion, P., Monroy, M., Holliger, P., Boiron, M.C., Cathelineau, M., Wagner, F.E., Friedl, J. (1991): Gold bearing pyrites: A combined ion microprobe and Mössbauer spectrometry approach. *in* "Source, transport and deposition of metals". Pagel & Leroy, eds. Balkema, Rotterdam, 677-680.

Maslenitsky, I. (1944): On some cases of formation of dispersed gold segregations in iron sulfides. *Doklady Akademii Nauk, SSSR*, **45**, 405-408 (in Russian).

Mironov, A.G. & Geletiy, V.F. (1978): Study of gold distribution throughout synthetic pyrites using radiotracer ^{195}Au. *Doklady Akademii Nauk, SSSR*, **241**, 1428-1431 (in Russian).

Mironov, A.G., Tauson, V.L., Geletiy, V.F. (1987): Metallicity of bounding as a factor facilitating gold incorporation into sulfide minerals structures. *Doklady Akademii Nauk, SSSR*, **293**, 447-449 (in Russian).

Möller, P. (1994): Accumulation of gold on natural sulfides: the electrochemical function of arsenic in nature. *Geol. Jb.*, **D 100**, 639-660.

Mycroft, J.R., Bancroft, G.M., McIntyre, N.S., Lorimer, J.W. (1995): Spontaneous deposition of gold on pyrite from solutions containing Au(III) and Au (I) chlorides. Part I: A surface study. *Geochim. Cosmochim. Acta*, **59**, 3351-3365.

Perchuk, L.L. & Riabchikov, I.D. (1976): Phase Composition Correlation in Mineral Systems. Nedra, Moscow (in Russian).

Scaini, M.J., Bancroft, G.M., Knipe, S.W. (1997): An XPS, AES, and SEM study of the interactions of gold and silver chloride species with PbS and FeS_2: comparison to natural samples. *Geochim. Cosmochim. Acta*, **61**, 1223-1231.

Shaw, D.M. (1969): Evaluation of data. *in* "Handbook of Geochemistry, vol.1". K.H.Wedepohl, ed., Springer-Verlag, Berlin-Heidelberg-New York, 324-375.

Starling, A., Gilligan, J.M., Carter, A.H.C., Foster, R.P., Saunders, R.A. (1989): High-temperature hydrothermal precipitation of precious metals on the surface of pyrite. *Nature*, **340**, 298-300.

Tauson, V.L. (1989a): The problem of phase composition correlation of real crystals in mineral systems. *in* "Mineralogy: Reports of Soviet Geologists at XXVIII Session of International Geological Congress". N.V. Sobolev *et al.*, eds. Nauka, Moscow, 77-84 (in Russian).

— (1989b): Surface free energy and growth morphology of pyrite and galena crystals. *Mineralogicheskii Zhurnal*, **11**, 30-39 (in Russian).

Tauson, V.L. & Akimov, V.V. (1986): Use of digenite ($Cu_{2-x}S$) for determination of sulfur fugacity in hydrothermal experiments. *Geokhimiya*, **10**, 1511-1513 (in Russian).

—, — (1991): Effect of crystallite size on solid state miscibility: Applications to the pyrite-cattierite system. *Geochim. Cosmochim. Acta*, **55**, 2851-2859.

Tauson, V.L. & Chernyshev, L.V. (1981): Experimental Study on Crystal Chemistry and Geochemistry of Zinc Sulfide. Nauka, Novosibirsk (in Russian).

Tauson, V.L. & Smagunov, N.V. (1997): Effect of gold-accompanying elements on gold behavior in the Fe-S-aqua-salt solution system at 450°C and 100 MPa. *Russian Geol. Geophys.*, **38**, 706-713.

Tauson, V.L., Mironov, A.G., Bugaeva, N.G., Pastushkova, T.M. (1998): The method to appreciate incorporation limits of gold in minerals. *Geologia i Geofizika*, **39**, 621-626 (in Russian).

Tyurin, N.G. (1965): On finely dispersed gold in pyrite. *Geologia Rudnykh Mestorozhdenii*, **7**, 70-75 (in Russian).

Voitzechovskiy, V.N., Berkovskiy, B.P., Yaschurzhinskaya, O.A., Chugaev, L.V., Nikitin, M.V. (1975): On the question of "invisible" gold occurrence in arsenopyrite and pyrite. *Izvestia Vysshych Uchebnych Zavedenii. Tzvetnayia Metallurgiya*, **3**, 60-65 (in Russian).

Zhang, Zhenru, Yang, Sixue, Yi, Wen (1987): Studies of submicro-gold and lattice-gold in some minerals. *J. Central-South Inst. Min. Metal.*, **18**, 355-361.

Received 4 December 1998
Modified version received 27 April 1999
Accepted 25 May 1999